DAVID W. TAYLOR
NAVAL SHIP RESEARCH AND DEVELOPMENT CENTER

Bethesda, Md. 20084
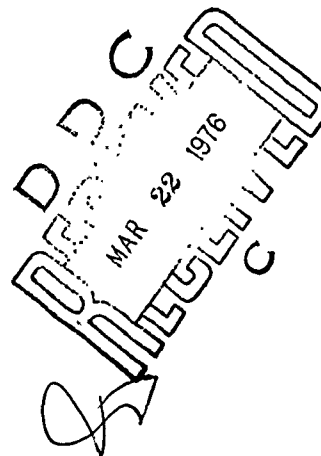
THE PERFORMANCE GAINS OF USING WIDE, FLUSH BOUNDARY LAYER INLETS ON WATER-JET PROPELLED CRAFT

by

John G. Purnell

PROPULSION AND AUXILIARY SYSTEMS DEPARTMENT

Annapolis

RESEARCH AND DEVELOPMENT REPORT

March 1976

MAJOR NSRDC ORGANIZATIONAL COMPONENTS

```
                        ┌─────────────────────┐
                        │      NSRDC          │
                        │   COMMANDER    00    │
                        │ TECHNICAL DIRECTOR 01│
* REPORT ORIGINATOR     └─────────────────────┘

┌─────────────────────┐              ┌─────────────────────┐
│  OFFICER-IN-CHARGE   │              │  OFFICER-IN-CHARGE  │
│   CARDEROCK    05    │              │   ANNAPOLIS    04   │
└─────────────────────┘              └─────────────────────┘

       ┌─────────────────────┐
       │      SYSTEMS         │
       │   DEVELOPMENT        │
       │   DEPARTMENT    11   │
       └─────────────────────┘

┌─────────────────────┐              ┌─────────────────────┐
│  SHIP PERFORMANCE    │              │    AVIATION AND     │
│   DEPARTMENT    15   │              │  SURFACE EFFECTS    │
└─────────────────────┘              │   DEPARTMENT    16  │
                                     └─────────────────────┘

┌─────────────────────┐              ┌─────────────────────┐
│    STRUCTURES        │              │   COMPUTATION       │
│   DEPARTMENT    17   │              │  AND MATHEMATICS    │
└─────────────────────┘              │   DEPARTMENT    18  │
                                     └─────────────────────┘

┌─────────────────────┐              ┌─────────────────────┐
│   SHIP ACOUSTICS     │              │ PROPULSION AND   *  │
│   DEPARTMENT    19   │              │ AUXILIARY SYSTEMS   │
└─────────────────────┘              │   DEPARTMENT    27  │
                                     └─────────────────────┘

┌─────────────────────┐              ┌─────────────────────┐
│     MATERIALS        │              │     CENTRAL         │
│   DEPARTMENT    28   │              │  INSTRUMENTATION    │
└─────────────────────┘              │   DEPARTMENT    29  │
                                     └─────────────────────┘
```

REPORT DOCUMENTATION PAGE	READ INSTRUCTIONS BEFORE COMPLETING FORM

1. REPORT NUMBER	2. GOVT ACCESSION NO.	3. RECIPIENT'S CATALOG NUMBER
PAS-75-45		

4. TITLE (and Subtitle)	5. TYPE OF REPORT & PERIOD COVERED
THE PERFORMANCE GAINS OF USING WIDE, FLUSH BOUNDARY LAYER INLETS ON WATER-JET PROPELLED CRAFT.	Research & Development
	6. PERFORMING ORG. REPORT NUMBER

7. AUTHOR(s)	8. CONTRACT OR GRANT NUMBER(s)
John G. Purnell	SF43-432-702

9. PERFORMING ORGANIZATION NAME AND ADDRESS	10. PROGRAM ELEMENT, PROJECT, TASK AREA & WORK UNIT NUMBERS
David W. Taylor Naval Ship R&D Center Annapolis, Maryland 21402	TA SF43432 S4622 Element 62543N & 63508N WU 2721-152 & 2721-155

11. CONTROLLING OFFICE NAME AND ADDRESS	12. REPORT DATE
David W. Taylor Naval Ship R&D Center Bethesda, Maryland 20084	March 1976
	13. NUMBER OF PAGES
	44

14. MONITORING AGENCY NAME & ADDRESS(if different from Controlling Office)	15. SECURITY CLASS. (of this report)
45 p.	Unclassified
	15a. DECLASSIFICATION/DOWNGRADING SCHEDULE

16. DISTRIBUTION STATEMENT (of this Report)

Approved for public release; distribution unlimited.

17. DISTRIBUTION STATEMENT (of the abstract entered in Block 20, if different from Report)

18. SUPPLEMENTARY NOTES

19. KEY WORDS (Continue on reverse side if necessary and identify by block number)

Performance gains
Boundary layer inlets
Water-jet propelled craft
Boundary layer conditions
Pump size

Water-jet performance

20. ABSTRACT (Continue on reverse side if necessary and identify by block number)

The application of a wide, flush inlet on a water-jet-propelled craft was investigated to determine performance gains from using primarily low momentum boundary layer flow for producing the propulsion jet. A method of predicting the boundary layer conditions, the pump size, and the overall water-jet system performance is given. Improvement in overall system efficiency or

(over)

DD FORM 1473 1 JAN 73   EDITION OF 1 NOV 65 IS OBSOLETE
S/N 0102-014-6601

20.   ABSTRACT (Cont)

propulsive coefficient of 10% to 12% over conventional flush
inlets is predicted for a planing craft application.

(Author)

ADMINISTRATIVE INFORMATION

LIST OF ABBREVIATIONS

DWDI - double width, double inlet

fps   - feet per second

gpm   - gallons per minute

lb/hp - pounds per horsepower

psf   - pounds per square foot

rpm   - revolutions per minute

TABLE OF CONTENTS

NOMENCLATURE

A_i	- Inlet area	ft^2
A_p	- Projected hull area	ft^2
C_c	- Cavitation coefficient	
C_{D_i}	- Inlet drag coefficient	
C_w	- Weight coefficient	
D_i	- Inlet drag	lb
D_s	- Shaft diameter	ft
D_{T_1}	- Pump inlet diameter	ft
D_{T_2}	- Pump exit diameter	ft
F_∇	- Froude number	
g	- Acceleration of gravity	ft/sec^2
$h_{e\ell}$	- Inlet submergence head	ft
h_v	- Vapor pressure	ft
H_i	- Inlet height	ft
H_{o_d}	- Off design pump head	ft
H_p	- pump head	ft
H_{p_d}	- design pump head	ft
K_e	- Energy velocity ratio (U_e/V_∞)	
K_ℓ	- Inlet loss coefficient	
K_m	- Momentum velocity ratio (U_m/V_∞)	
K_1	- Pump efficiency parameter	sec^2/ft^5
K_2	- Pump efficiency parameter	sec^3/ft$^{15/2}$
L_w	- Inlet width	ft
L_x	- Wetted hull length upstream of inlet	ft
n	- Exponent	
N	- Pump speed	rpm

N_p - Number of pumps

N_{p_i} - Number of pump inlets

N_s - Specific speed $\text{rpm}\cdot\text{gpm}^{1/2}/\text{ft}^{3/4}$

NPSH - Net positive suction head   ft

P_{atm} - Atmospheric pressure head   ft

$P_{b\ell}$ - Boundary layer net thrust pressure   psf

P_i - Input power   ft-lb/sec

Q   - Flow rate   cfs

Q_d - Design flow rate   cfs

Q_{o_d} - Off design pump flow rate   cfs

Q_{imp} - Flow per impeller inlet   gpm

R   - Jet velocity ratio (V_j/V_∞)

R_c - Craft resistance at design displacement   lb

R_{c_o} - Craft resistance at reduced displacement   lb

Re   - Reynolds number

S   - Integral number of pump stages

sfc   - Specific fuel consumption   lb/hp-hr

T_c - Craft or gross thrust   lb

T_{net} - Net thrust   lb

U   - Local velocity at distance y from hull   fps

U_a - Average velocity of ingested flow   fps

U_e - Energy velocity of ingested flow   fps

U_m - Momentum velocity of ingested flow   fps

U_{t_1} - Pump inlet tip speed   fps

U_{t_2} - Pump exit tip speed   fps

V_{ax} - Pump axial inlet velocity   fps

V_i - Average inlet velocity   fps

V_j	- Jet velocity	fps
V_∞	- Free stream or craft velocity	fps
W_{ap}	- Axial pump weight	lb
W_c	- Craft design weight	lb
W_{c_o}	- Craft weight at reduced displacement	lb
W_{c_p}	- Centrifugal pump weight	lb
y	- Distance from hull	ft
L/B	- Craft length to beam ratio	
U/V_∞	- Local velocity ratio	
y/δ	- Height ratio	

α	- Inlet velocity ratio (V_i/V_∞)	
δ	- Boundary layer thickness	ft
∇	- Craft displacement at rest	ft^3
η_o	- Overall efficiency or propulsive coefficient	
η_p	- Pump efficiency	
η_{po_d}	- Off design pump efficiency	
η_t	- Transmission efficiency	
λ	- Shaft blockage coefficient (D_s/D_{t_1})	
ν	- Viscosity of seawater	ft^2/sec
ρ	- Density of seawater	$slugs/ft^3$
σ_t	- Thoma cavitation number	
τ	- Energy ratio based on V_{ax}	
τ_u	- Energy ratio based on U_{t_1}	
$\emptyset$	- Flow coefficient	

INTRODUCTION

Water-jet propulsion systems have found increased application on many types of naval ships, such as surface effect ships, hydrofoils, and planing craft. The attractiveness of the water-jet system lies mostly in its high reliability and basic simplicity compared to alternative systems. The main disadvantage has been that the performance coefficient or overall efficiency of water-jet systems may be on the order of 10% lower than that of propeller-type systems.

Improvements are desired which will permit the overall efficiency of typical water-jet systems to approach more closely those of propeller systems. In the area of planing hull craft it appears possible to approach propeller system efficiencies by making use of the low momentum fluid in the craft boundary layer near the stern to reduce the inflow momentum drag of the water-jet system. This requires that a wide or large width/height ratio inlet be used, spanning as much of the beam as possible in order to minimize the inlet height such that flow would be drawn primarily or entirely from the boundary layer. Planing-type craft have sufficient beam for the flow rates required to make wide boundary layer inlets feasible.

This report considers the application of wide boundary layer inlets to water-jet-propelled craft where maximum craft velocities are on the order of 50 knots. Special attention is given to planing craft since they have sufficient beam and high speed; however, results are applicable to displacement vessels.

WIDE BOUNDARY LAYER INLETS

The application of water-jet propulsion to displacement craft offers important advantages in addition to reliability and simplicity when compared to a propeller system:

- Shallow draft capability.

- Elimination of propulsion system damage from striking underwater objects.

- Reduction of appendage drag.

With the use of a wide boundary layer inlet, where water-jet flow is drawn primarily or entirely from the boundary layer, several other advantages are possible:

- System efficiency can, in some cases, approach or exceed that of a propeller system.

- Amount of inflow diffusion required for the flow (as well as diffuser size) is reduced.

- Inlet drag can be reduced.

Some potential problem areas do exist with wide boundary layer inlets. The distorted boundary layer flow profile coming into the inlet makes efficient diffusion without separation difficult. Because the inlet is very wide and the inlet height is thus very small, the length of diffuser required for a given diffusion ratio will be very short, thus minimizing additional losses, since the pump may be placed physically very close to the inlet. Machinery arrangement can be a problem. If the wide inlet flow is diffused to one (or two) pumps, the diffusion would be three-dimensional, and the transition of diffuser and duct shape between inlet and pump would cause high internal losses. However, it appears that a satisfactory pumping arrangement is obtained with multiple small diameter impellers (i.e., DWDI* centrifugal) mounted in parallel across the beam of the craft on a common shaft as shown in figure 1. With this arrangement the diffusion remains essentially two-dimensional.

FORWARD
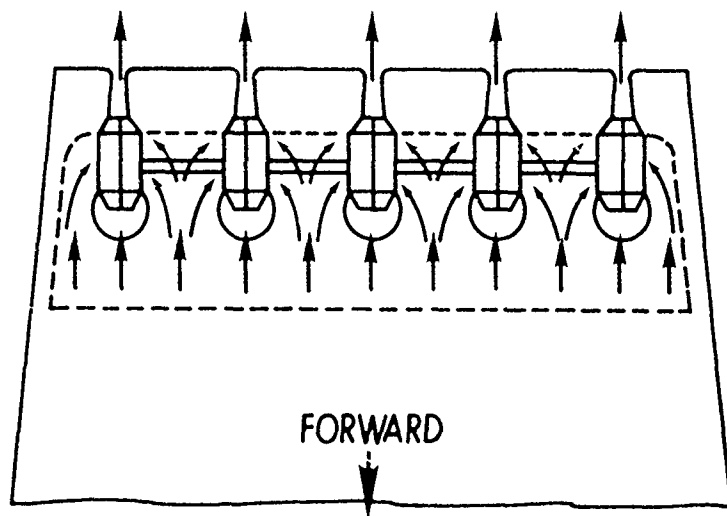
Figure 1
Wide Boundary Layer
Inlet Using Multiple,
Parallel, Double
Width, Double Inlet
Centrifugal Pumps

FORWARD

---
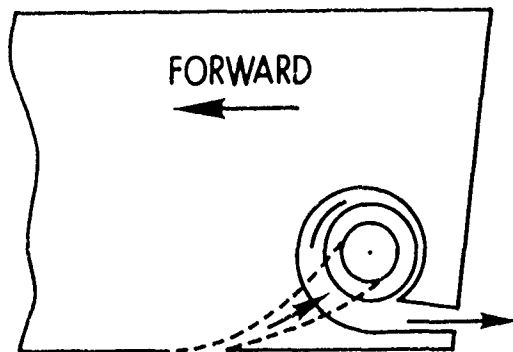
*Definitions of abbreviations are on page i.

A major problem with this arrangement is the power transmission to the athwartship mounted pump shaft. Another problem area of the wide inlet appears to be the ingestion of debris into the system. Many present inlet systems use inlet grates to block objects from entering the system. How some arrangement such as this would affect a wide boundary layer inlet is presently unknown. Air ingestion, especially in turning maneuvers, is also a potential problem that could significantly limit inlet width. Model tests to determine the magnitude of these problem areas and practical solutions will be needed to fully pursue the application of this concept to high performance planing craft.

The analysis approach used in this report was first to determine empirical methods for calculating boundary layer thickness and profile at the inlet. With this information the velocities at the inlet can then be determined for any given set of conditions and performance predicted.

<div align="center">BOUNDARY LAYER CHARACTERISTICS</div>

BOUNDARY LAYER THICKNESS

The successful design of a wide boundary layer inlet depends on having some knowledge of the boundary layer on the craft prior to the inlet. Based on test craft data[1-5], it is evident that the boundary layer thickness at any point along the craft base can be approximated by Prandtl's equation for boundary layer thickness:

$$\frac{\delta}{L_x} = 0.376 * \left(\frac{V_\infty L_x}{\nu}\right)^{-1/5} = 0.376 \, Re^{-1/5}, \tag{1}$$

where Re = Reynolds number = $V_\infty L_x/\nu$. (1a)

The boundary layer thickness, δ, varies inversely as the 1/5-power of the free stream velocity. Thus, boundary layer thickness decreases with increasing craft speed.

The above equation for boundary layer thickness is applicable basically only to the zero pitch case. It has been shown that craft pitch has considerable effect on the boundary layer.[3,5]

---

[1]Superscripts refer to similarly numbered entries in the Technical References at the end of the text.

a 3-degree bow-up pitch resulted in a 40% reduction in boundary layer thickness during model tests.[3] In the zero pitch case, drag is primarily frictional, while in the bow-up pitch, drag has both frictional and pressure components. However, with increasing trim or pitch angle, the bottom pressure is greater than the free stream pressure because the average bottom velocity is less than the forward speed by Bernoulli's equation. Additional study or experimentation will be necessary to determine the boundary layer characteristics of different types of craft, especially planing craft, which are designed with some amount of bow-up pitch. However, equation (1) will be assumed to be applicable, except in extreme cases, since it has shown agreement with experimental craft data.[1-5]

BOUNDARY LAYER PROFILES

Details of the boundary layer profile are required for determining the average, momentum, and energy velocities of the flow into the inlet. The characteristic boundary layer shapes are assumed to have an exponential boundary layer profile described by:

$$\frac{U}{V_\infty} = \left(\frac{y}{\delta}\right)^{1/n} \qquad \text{For } \frac{y}{\delta} \leq 1, \qquad (2)$$

where

$$n = \log_{10} Re \qquad (3)$$

Figure 2 shows the effect of the value of the exponent n on the shape of the boundary layer profile. Increasing n increases the local velocity ratio, U/V_∞, for any given height ratio, y/δ.

The distance, y, is the depth below the hull from which flow is ingested, as shown in figure 3, and defines the dividing streamline between flow into the inlet and around it. The average velocity in the ingested flow is calculated from:

$$\frac{U_a}{V_\infty} = \frac{\delta}{y} \int_0^{(y/\delta)} \frac{U}{V_\infty} d\left(\frac{y}{\delta}\right). \qquad (4)$$
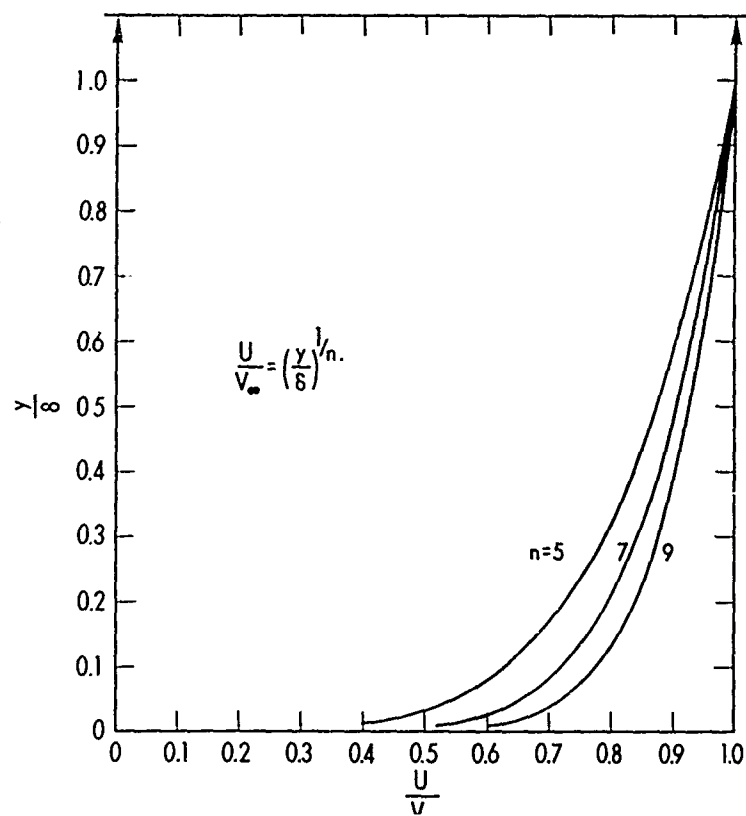
$$\frac{U}{V_\infty} = \left(\frac{y}{\delta}\right)^{1/n}.$$

Figure 2 - Boundary Layer Profiles as a
Function of the Power n

DIVIDING STREAMLINE BETWEEN
FLOW INTO THE INLET AND
AROUND IT

WHERE:
U_A = AVERAGE VELOCITY OF INGESTED FLOW
U_M = MOMENTUM VELOCITY OF INGESTED FLOW
U_E = ENERGY VELOCITY OF INGESTED FLOW
U = LOCAL VELOCITY AT DIVIDING STREAMLINE
V_∞ = FREE STREAM VELOCITY
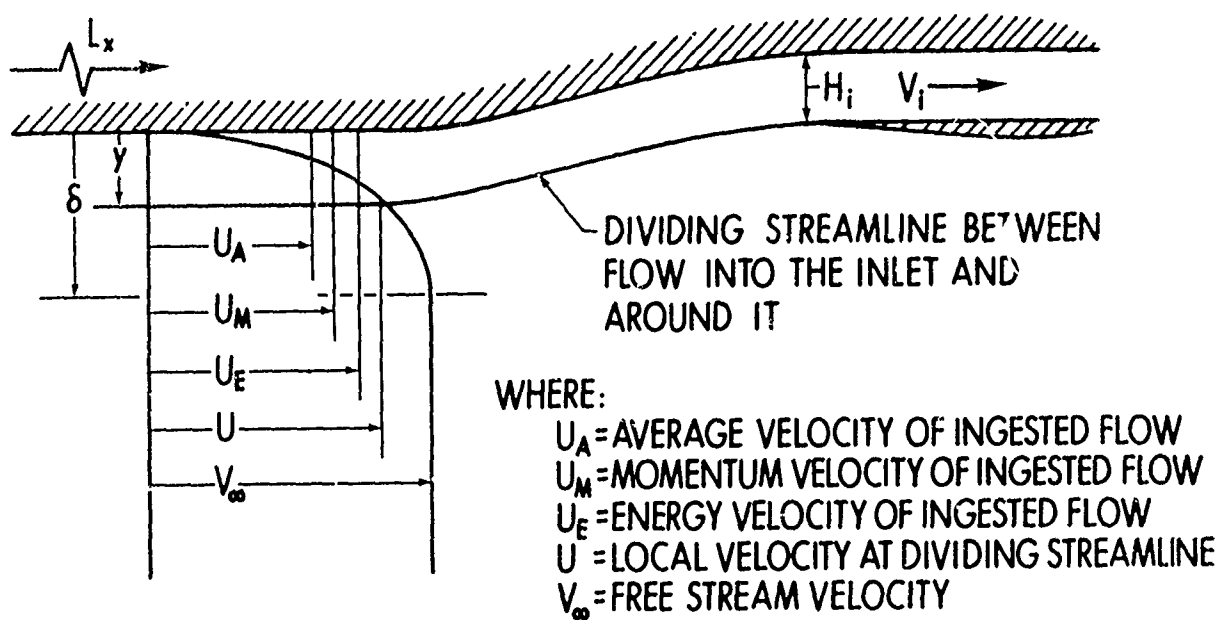
Figure 3 - Wide Inlet and Boundary Layer

The momentum velocity of the ingested flow is obtained from:

$$\frac{U_m}{V_\infty} = \frac{V_\infty}{U_a} \frac{\delta}{y} \int_0^{(y/\delta)} \left(\frac{U}{V_\infty}\right)^2 d\left(\frac{y}{\delta}\right).$$ (5)

The energy velocity of the ingested flow is calculated from:

$$\frac{U_e}{V_\infty} = \left(\frac{V_\infty}{U_a} \frac{\delta}{y} \int_0^{(y/\delta)} \left(\frac{U}{V_\infty}\right)^3 d\left(\frac{y}{\delta}\right)\right)^{1/2}.$$ (6)

The local velocity ratio, U/V_∞, at the dividing streamline is obtained from equation (2) for $y/\delta \leq 1$; however, for $y/\delta > 1$, equations (4), (5), and (6) must be integrated over the additional interval of 1 to y/δ, where the local velocity ratio is equal to one at all points.

The exponential boundary layer profile of equation (2) and the basic definition of equations (4), (5), and (6) may be used to derive the following equations:

For $y/\delta \leq 1$,

$$\frac{U_a}{U} = \frac{n}{n + 1}$$ (7a)

$$\frac{U_m}{U} = \frac{n + 1}{n + 2}$$ (7b)

$$\frac{U_e}{U} = \left(\frac{n + 1}{n + 3}\right)^{1/2}$$ (7c)

For $y/\delta > 1$,

$$\frac{U_a}{V_\infty} = 1 - \frac{1}{\left(\frac{y}{\delta}\right)(n + 1)}$$ (8a)

$$\frac{U_m}{V_\infty} = \frac{(\frac{y}{\delta}) - 1 + \frac{n}{(n + 2)}}{(\frac{y}{\delta}) - \frac{1}{(n + 1)}} \tag{8b}$$

$$\frac{U_e}{V_\infty} = \left(\frac{(\frac{y}{\delta}) - 1 + \frac{n}{(n + 3)}}{(\frac{y}{\delta}) - \frac{1}{(n + 1)}} \right)^{1/2}. \tag{8c}$$

The value $y/\delta > 1$ indicates that flow is also taken from beyond the boundary layer. The exponential boundary layer of equation (2) and the basic definitions of the velocities shown in figure 3 may be used to relate the local height ratio at the dividing streamline to the inlet conditions by:

$$\frac{y}{\delta} = \left(\frac{U}{V_\infty} \right)^n = \left[\left(\frac{V_i}{V_\infty} \right) \left(\frac{H_i}{\delta} \right) \left(\frac{n + 1}{n} \right) \right]^{n/(n + 1)} \quad \text{For } \frac{y}{\delta} \le 1 \tag{9a}$$

and

$$\frac{y}{\delta} = \left[\frac{1}{(n + 1)} + \left(\frac{V_i}{V_\infty} \right) \left(\frac{H_i}{\delta} \right) \right] \quad \text{For } \frac{y}{\delta} > 1. \tag{9b}$$

PERFORMANCE OF BOUNDARY LAYER INLETS

In calculating the performance of a water-jet system, it is a normal first assumption to neglect the effects of the boundary layer. However, the boundary layer reduces the momentum and energy velocities at the inlet and is a most important factor to consider for this concept. Burke, et al,[1] showed the momentum velocity for the XR-1B inlet was about 0.935 times the free stream velocity.

The craft or gross thrust, T_C, is calculated from:

$$T_C = \rho \, Q \, (V_j - U_m)$$

$$= \rho \, Q \, V_\infty (R - K_m).$$ (10)

The drag of the inlet, D_i, is obtained from:

$$D_i = \frac{\rho}{2} \, C_{D_i} \, A_i \, V_\infty^2 = \rho \, V_\infty \, Q \, \frac{C_{D_i}}{2\alpha}.$$ (11)

The net thrust T_{net} required by the craft is obtained by subtracting the inlet drag from the craft thrust requirement; thus:

$$T_{net} = T_C - D_i$$

$$= \rho \, V_\infty \, Q \left(R - K_m - \frac{C_{D_i}}{2\alpha} \right).$$ (12)

The required input power P_i, is given by:

$$P_i = \rho \, Q \left(\frac{V_j^2}{2} - \frac{U_e^2}{2} + K_\ell \, \frac{U_e^2}{2} \right) \frac{1}{n_p \, n_t}$$

$$= \rho \, Q \, \frac{V_\infty^2}{2} \left(R^2 + K_e^2 \, (K_\ell - 1) \right) \frac{1}{n_p \, n_t}.$$ (13)

The overall efficiency or propulsive coefficient, n_O, of the water-jet system is obtained by use of equations (12) and (13), giving:

$$n_O = \frac{T_{net} \, V_\infty}{P_i}$$

$$= \frac{2 \left(R - K_m - \frac{C_{D_i}}{2\alpha} \right)}{R^2 + K_e^2 \, (K_\ell - 1)} \, n_p \, n_t.$$ (14)

The effects of boundary layer flow ingestion on the overall efficiency are shown in figures 4 through 6. Reducing the momentum velocity ratio for any jet velocity ratio increases the overall efficiency of the water-jet system. Increasing the drag coefficient and/or system loss coeffic.ent reduces the overall efficiency as would be expected. The effects of the value of n from equation (3) on the overall efficiency were negligible since the energy velocity ratios calculated for the different ɔ's were very close for a constant momentum velocity ratio. With reducing momentum velocity ratio, the point of peak overall efficiency is shifted to lower jet velocity ratios. Increasing jet velocity ratio minimizes the gains due to boundary layer ingestion since jet velocity now becomes the dominant term in the performance prediction equation (i.e., equations (10), (12), (13), and (14). Thus, a wide inlet system should have a low design jet velocity ratio, approximately 1.6 to 2.0, and is most applicable to a craft that spends a large percentage of its time at or near its design jet velocity ratio, which implies high craft speed. At low speed where the jet velocity ratio is high, the wide inlet system has performance that is comparable to that of the conventional flush inlet.
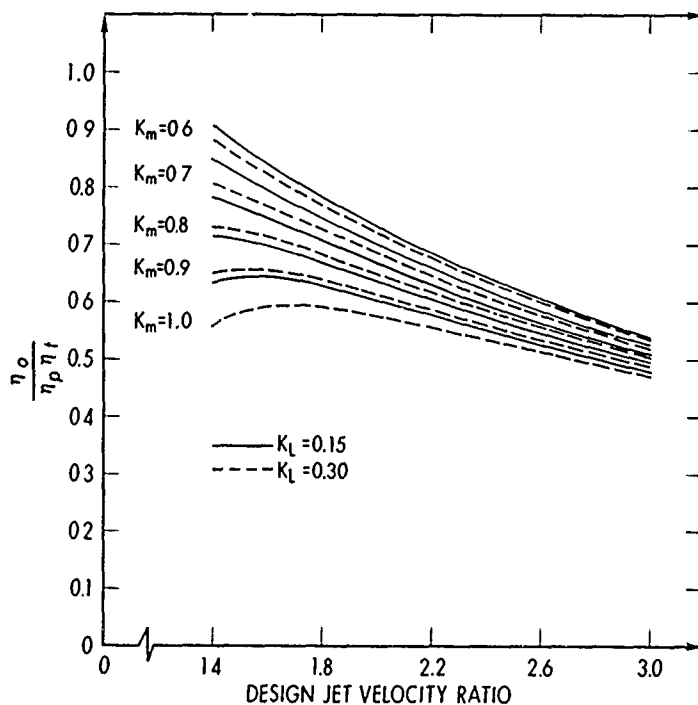

Figure 4 - Effects of Boundary Layer Flow
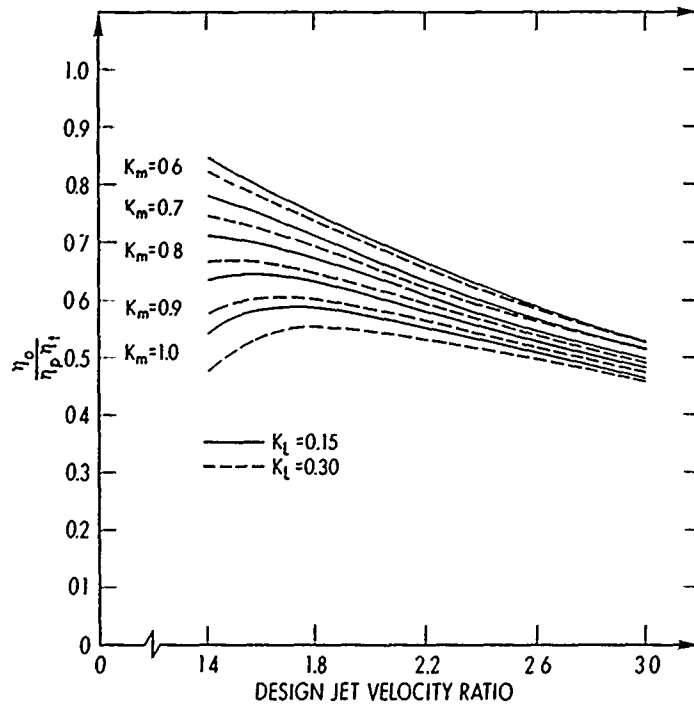Ingestion on the Overall Efficiency
for $C_{D_i}/2\alpha = 0.05$

Figure 5 - Effects of Boundary Layer Flow
Ingestion on the Overall Efficiency
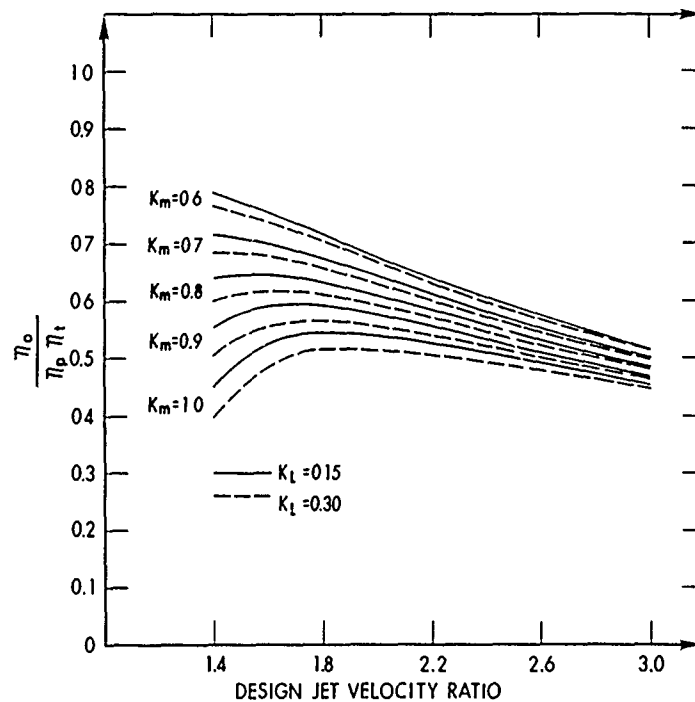for $C_{D_i}/2\alpha = 0.1$

Figure 6 - Effects of Boundary Layer Flow
Ingestion on the Overall Efficiency
for $C_{D_i}/2 = 0.15$

By equating the net thrust equation at constant flow and velocity for two different K_m values, the following is obtained:

$$R' = R - (K_m - K_m') - \frac{\left(c_{D_i} - c_{D_i}'\right)}{2\alpha} , \qquad (15)$$

with the primed quantities denoting conditions at the second K_m value. Thus, if the system is designed for a lower K_m value (i.e., wider inlet), it is possible to reduce the jet velocity ratio for the same flow rate and thus have approximately the same size system. The inlet drag coefficient will decrease slightly with decreasing K_m, but its effect in equation (15) will be at least an order of magnitude less than the effects of the K_m term and may be ignored. Thus, the reduction in jet velocity ratio with decreasing K_m can improve efficiency both by minimizing energy lost in the jet and by reduced inlet momentum losses.

WIDE BOUNDARY LAYER INLET DESIGN

The size of the wide boundary layer inlet will depend on several factors, the most important being the available hull width near the transom of the craft that is suitable for inlet use. Not all of this width can be used since such problems as avoiding broaching in turns can reduce available width. The flow into the inlet can be determined from the net thrust equation (12) by:

$$Q = \frac{T_{net}}{\rho\, V_\infty \left(R - K_m - \frac{c_{D_i}}{2\alpha}\right)} . \qquad (16)$$

The flow rate into the inlet can also be determined from any of the following:

$$Q = U_a\, y\, L_w \qquad (17a)$$

$$Q = H_i\, V_i\, L_w \qquad (17b)$$

$$Q = H_i\, \alpha\, V_\infty\, L_w . \qquad (17c)$$

If flow is assumed to be taken from the boundary layer region or from the boundary layer region and beyond, then by substitution from equations (2), (4), (7a), (7b), and (8a) in (17a) the following expressions for flow are obtained, respectively:

$$Q = \frac{n}{n+1} V_\infty \, \delta \, L_W \left[\frac{n+2}{n+1} K_m\right]^{n+1} \qquad \left(\text{For } \frac{y}{\delta} \leq 1\right) \qquad (18a)$$

and

$$Q = V_\infty \, \delta \, L_W \left[\frac{y}{\delta} - \frac{1}{n+1}\right] \qquad \left(\text{For } \frac{y}{\delta} > 1\right). \qquad (18b)$$

y/δ in equation (18b) may be expressed in terms of K_m and n using equation (8b). Equating (16) with (18a) and (18b), the inlet width can be calculated from:

$$L_W = \frac{T_{net}}{\dfrac{\rho \, V_\infty^2 \, \delta \, n}{n+1} \left[\dfrac{n+2}{n+1} K_m\right]^{n+1} \left[R - K_m - \dfrac{C_{D_i}}{2\alpha}\right]} \qquad \left(\text{For } \frac{y}{\delta} \leq 1\right). \qquad (19a)$$

and

$$L_W = \frac{T_{net}}{\rho \, V_\infty^2 \, \delta \left[\dfrac{y}{\delta} - \dfrac{1}{n+1}\right] \left[R - K_m - \dfrac{C_{D_i}}{2\alpha}\right]} \qquad \left(\text{For } \frac{y}{\delta} > 1\right). \qquad (19b)$$

Thus, for a given available inlet width, a range of jet velocity and inlet momentum velocity ratios exist that will satisfy the equations. If the jet velocity ratio is fixed, there will be a minimum inlet momentum velocity ratio below which there is not sufficient inlet width available. Equations (19a) and (19b) may be rewritten to express what will be called a boundary layer net thrust pressure, $P_{b\ell}$, where:

$$P_{b\ell} = \frac{T_{net}}{L_W \, \delta} = \frac{\rho \, V_\infty^2 \, n}{n+1} \left[\frac{n+2}{n+1} K_m\right]^{n+1} \left[R - K_m - \frac{C_{D_i}}{2\alpha}\right] \quad \left(\text{For } \frac{y}{\delta} \leq 1\right) \quad (20a)$$

$$P_{b\ell} = \frac{T_{net}}{L_W \, \delta} = \rho \, V_\infty^2 \left[\frac{y}{\delta} - \frac{1}{n+1}\right] \left[R - K_m - \frac{C_{D_i}}{2\alpha}\right] \quad \left(\text{For } \frac{y}{\delta} > 1\right). \quad (20b)$$

The net boundary layer thrust pressure is plotted in figures 7
and 8 as a function of jet velocity ratio for different inlet
momentum velocity ratios at 50 and 25 knots, respectively. The
n value is representative of the range of Reynolds numbers to be
expected. With the basic craft design information, the $P_{b\ell}$ value
can be calculated and will be constant for a given craft velocity.
If the value of $P_{b\ell}$ at 50 knots (which is about the maximum
velocity for a naval planing hull craft) is checked in figure 7,
the range of K_m values possible is shown. Decreasing jet velocity
ratio increases the minimum attainable K_m value and the size
and weight of the system since flow rates increase significantly.
The overall system efficiency will vary over the allowable K_m
range for a given $P_{b\ell}$, and the point of optimum efficiency may be
determined from equation (14) or thru figures 4, 5, and 6.
Increases in the value of $C_{D_i}/2\alpha$ in equations (20a) and (20b)
have only a slight effect in reducing $P_{b\ell}$ since its value is
small in comparison to the other terms.

Figure 7 – Boundary Layer
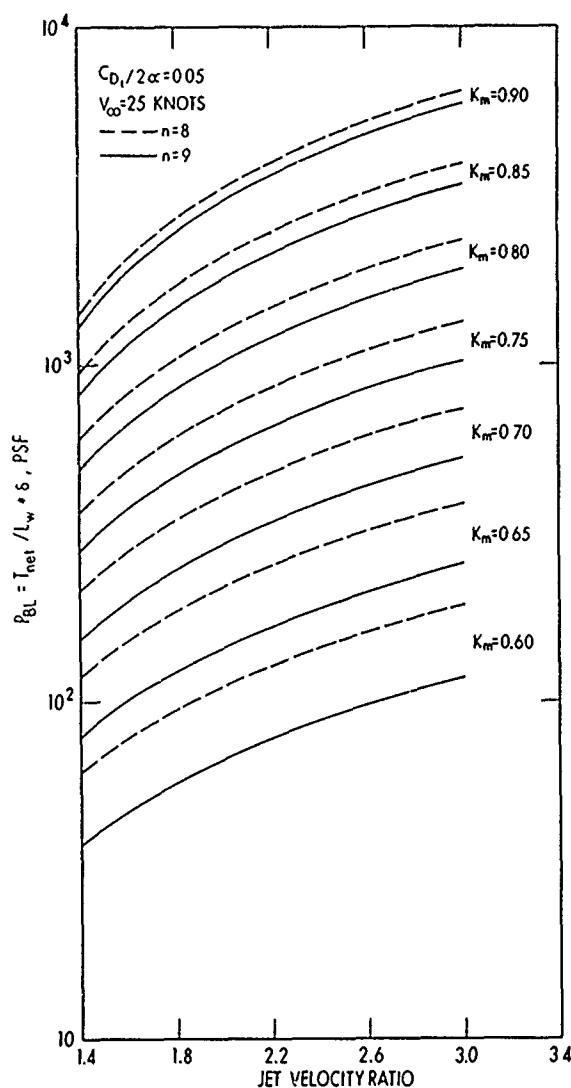Net Thrust Pressure
as a Function of R and K_m
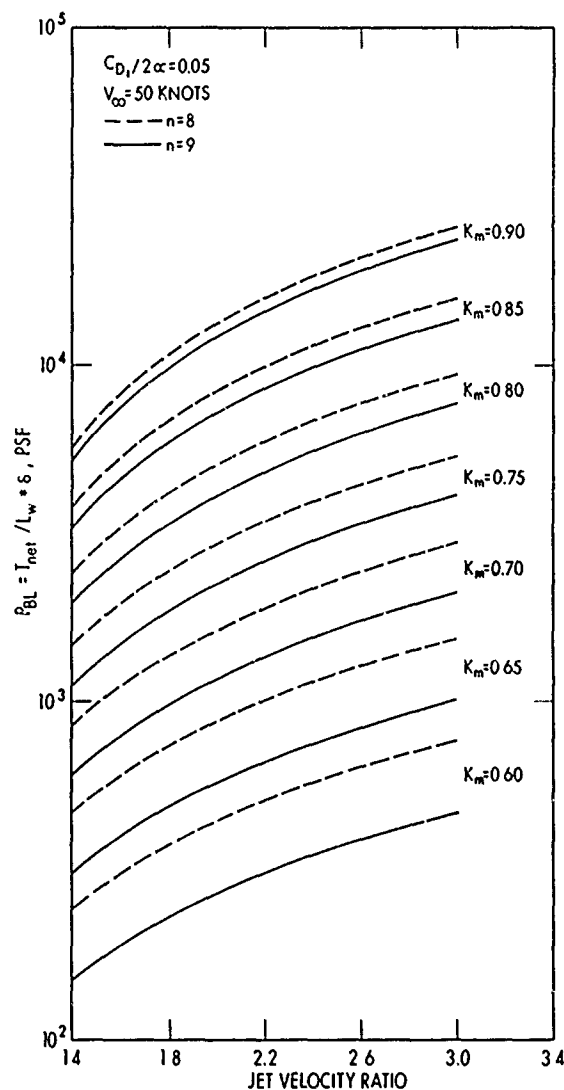
Figure 8 - Boundary Layer
Net Thrust Pressure
as a Function of R and K_m

CRAFT DRAG AND PART POWER OPERATION

As speed increases on a planing hull craft, a point will be reached where enough lifting force is generated by the hull form to start lifting some of the hull clear of the water, thus reducing wetted surface area and slowing the rate of drag increase. This effect causes a hump in the drag curve at the intermediate speeds. Figure 9 shows a plot of craft resistance or drag as a function of Froude number based on the following equation:[6]

$$\frac{R_C}{W_C} = 0.032 \ F_\nabla + 0.028 \ \sin^2\left(\frac{\pi \ F_\nabla}{5}\right) , \qquad (21)$$

where

$$F_\nabla = \text{Froude number} = \left(\frac{V_\infty}{\sqrt{g \; \nabla^{1/3}}}\right) \qquad (22)$$

$$\nabla = \frac{W_c}{\rho g} \qquad (23)$$

This equation is representative of planing craft in the 20- to 100-ton displacement range with 50-knot speed capability. For these conditions a length/beam ratio of 5.5 appears optimum and was assumed in estimating resistance above.[6] A load coefficient ($A_p/\nabla^{2/3}$) of 7.0 was chosen as representative of 20- to 100-ton craft in the development of equation (21).[6] The resistance values calculated by equation (21) are for a bare hull and have been increased by 25% to account for increased resistance due to such factors as appendages, roughness, and sea state.
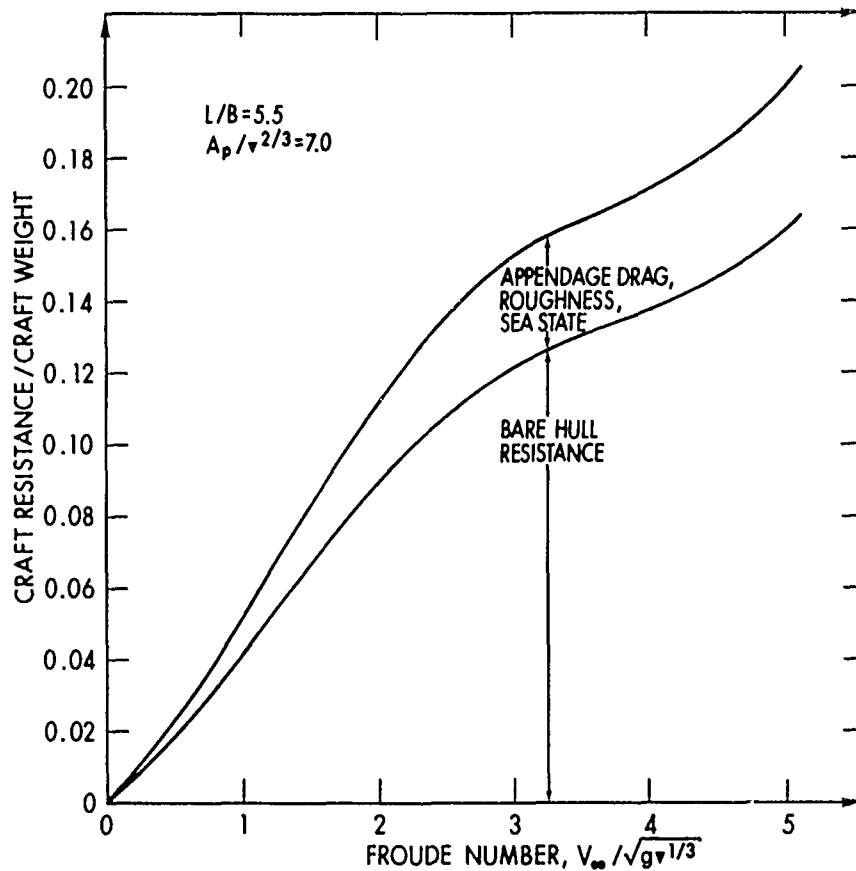

Figure 9
Craft Resistance versus Froude Number

Craft resistance at reduced displacement has been estimated by:

$$\left(\frac{R_{co}}{W_{co}}\right) = \frac{1}{2} \left(\frac{R_c}{W_c}\right) \left[1 + \frac{W_{co}}{W_c}\right] .$$ (24)

PUMP DESIGN

Axial and double inlet centrifugal pumps are both candidate systems for use with a wide boundary layer inlet. The double width, double inlet centrifugal pumps offer a good combination with the wide inlet since the pumps can be strung in parallel across the transom and mounted on a common shaft as in figure 1. Axial pumps with their high efficiency and light weight could provide an optimum system, and weight tradeoffs between different axial and centrifugal arrangements will be investigated later.

In the pump design, care must be taken to avoid cavitation at cruise conditions or pump life will be severely shortened. During periods of craft acceleration, some cavitation can be tolerated as long as it does not degrade pump performance, since the acceleration times are relatively short and no significant damage should result. The cavitation performance of a pump can be characterized by its flow coefficient, $\emptyset$, and the non-dimensionalized energy ratio, τ, where:

$$\emptyset = \frac{V_{ax}}{U_{t_1}}$$ (25)

and

$$\tau = \frac{NPSH}{V_{ax}^2/2g}$$ (26)

or

$$\tau_u = \frac{NPSH}{U_{t_1}^2/2g}$$ (26a)

where

$$NPSH = \frac{U_e^2}{2g} \left(1 - K_\ell\right) + P_{atm} + h_{e\ell} - hv$$ (27)

and

$$\tau_u = \phi^2 \tau .$$ (28)

There exist relationships between energy ratio and flow coefficient that can be used for determining cavitation performance. For cavitation free pump performance:

$$\tau \geq 1 + C_c (1 + 1/\phi^2)$$ (29)

$$\tau_u \geq \phi^2 + C_c (1 + \phi^2),$$ (30)

where

C_c = 0.3 for noncavitating flow in general

= 0.25 for noncavitating flow with well-designed pumps.

Since some cavitation can be tolerated under transient conditions, such as during acceleration and hump conditions, a smaller and lighter pump design is possible with limited cavitation. Based on data for axial[7] and centrifugal[8] pumps, expressions for energy ratio as a function of flow coefficient at 115% of breakdown NPSH yield over the given ranges of flow coefficient data:

For axial pumps,

$$\tau_u \geq 1.41 \, \phi^2 + 0.1129 \, \phi + 0.0130 \quad [0.07 \leq \phi \leq 0.23].$$ (31)

For centrifugal pumps,

$$\tau_u \geq 0.0195 + 0.86 \, \phi - 0.083 \phi^2 \quad [0.08 \leq \phi \leq 0.40].$$ (32)

For cruise conditions the pump must be cavitation free as defined by equations (29) and (30). However, for transient conditions, the pump can be allowed to operate down to the limits of equation (31) or (32).

Pump inlet tip speed, inlet diameters, and rpm are determined by:

$$U_{t_1} = \frac{2g \, NPSH}{\tau_u}^{1/2}$$ (33)

$$D_{t_1} = \left(\frac{4Q}{\pi (1 - \lambda^2) \, V_{ax} \, N_{p_i}} \right)^{1/2} \tag{34}$$

$$N = \frac{60}{\pi} \frac{U_{t_1}}{D_{t_1}} . \tag{35}$$

For axial pumps, an inducer stage plus additional stages can be used. The number of pump stages required is determined by:

$$S \geq \frac{4g \, H_p}{U_{t_1}^2} - 0.6 , \tag{36}$$

where S = least integral number of stages satisfying equation (36).

Axial pump weight, including water weight can be determined from the empirical relation:[9]

$$W_{ap} = [880 + 100 \, (S - 5)] \, D_{t_1}^{5/2} . \tag{37}$$

For centrifugal pumps the outlet diameter is determined from:[10]

$$D_{t_2} = \left[0.35 + \left(0.1225 + \frac{g \, H_p}{\eta_p \, U_{t_1}^2} \right)^{1/2} \right] D_{t_1} , \tag{38}$$

and DWDI centrifugal wet pump weight is determined from:[9]

$$W_{cp} = C_w \, N_s \, D_{t_2}^2 \, [0.725 \, N_p + 0.275] \, (1.55) , \tag{39}$$

where $C_w = 4.66$.

By combining equations (33), (34), and (35) and dividing by pump head, the following expression for specific speed is obtained:

$$N_s \equiv \frac{NQ_{imp}^{1/2}}{H_p^{3/4}} = 635.6 \left(\frac{2g \ \sigma_t}{\tau_u}\right)^{3/4} \left(\frac{(1 - \lambda^2)}{\pi} \emptyset\right)^{1/2} \tag{40}$$

where σ_t = Thoma cavitation number = $\dfrac{NPSH}{H_p}$.

Assuming $\lambda = 0.3$:

$$N_s = 7772 \ \frac{\emptyset^{1/2}}{\tau_u^{3/4}} \ \sigma_t^{3/4} . \tag{41}$$

Equation (41) is plotted in figures 10 through 12 for the non-cavitating and limited cavitating design cases defined by using the equalities in equations (30), (31), and (32), respectively. Thus, these figures represent upper limits on specific speed for a given Thoma number.

Pump designs are usually characterized by their specific speed, where:[9]

- $500 \le N_s \le 4,000$ for centrifugal pumps.

- $4,000 \le N_s \le 10,000$ for mixed flow pumps.

- $10,000 \le N_s \le 15,000$ for axial pumps.

Thus, for higher specific speed designs, figures 10 through 12 show that high Thoma cavitation numbers are required, meaning large NPSH and/or low pump head rise. However, with the increased application of inducers, the characteristic specific speeds of pumps can be reduced. Axial pump inducer stages can now be designed for specific speed as low as about 3500.
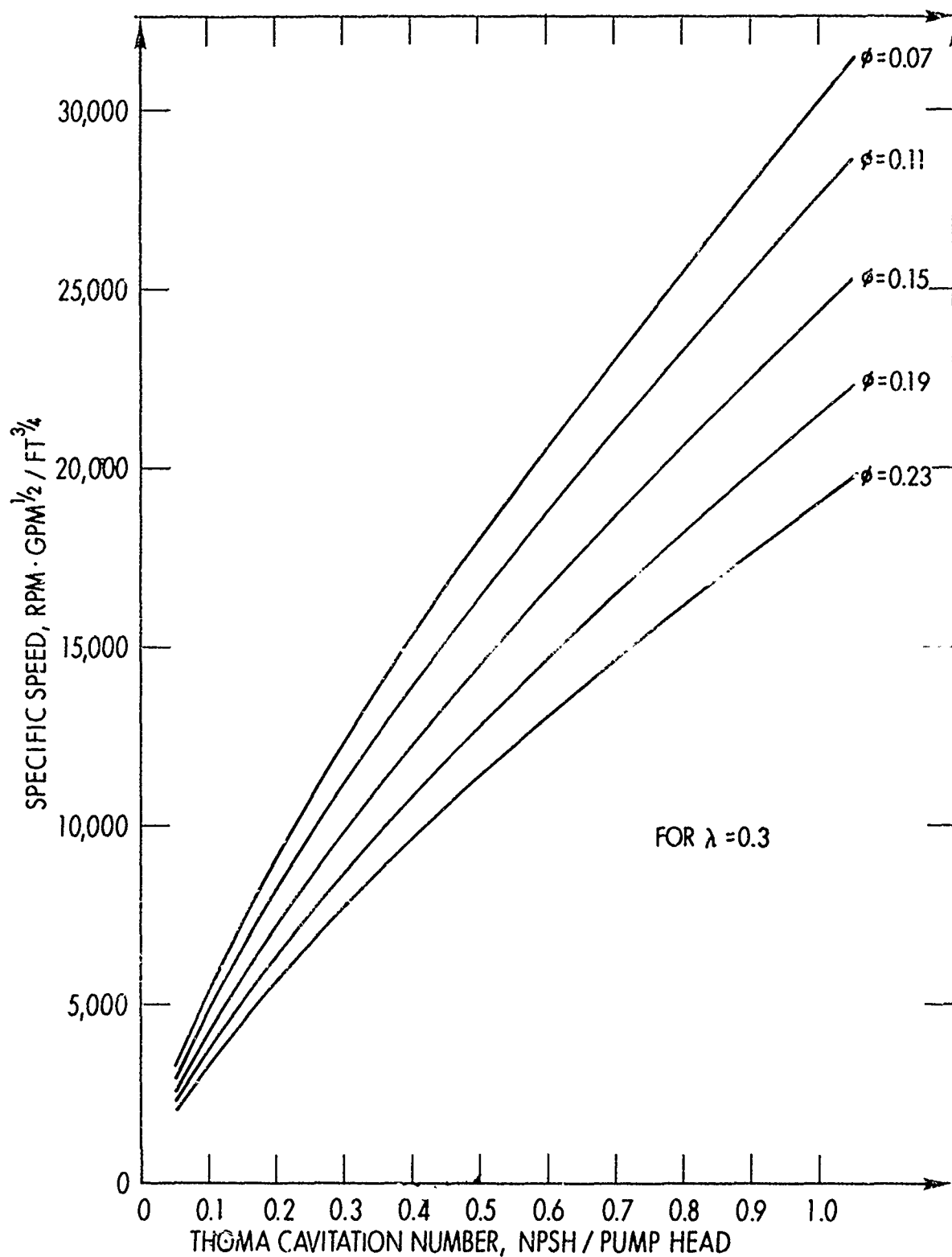
Figure 10
Axial Pump Specific Speed Versus Thoma Cavitation
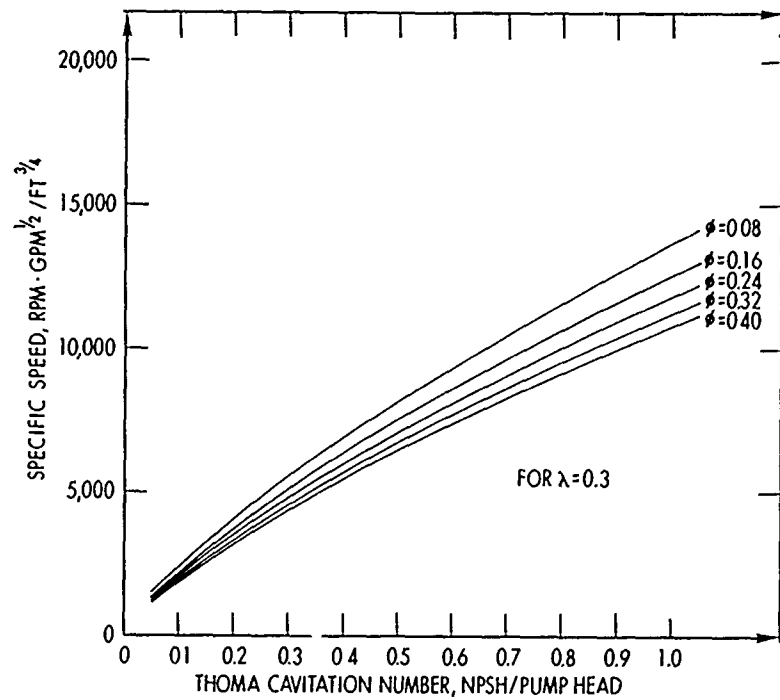Number for Limited Cavitating Designs

20

Figure 11
Centrifugal Pump Specific Speed Versus Thoma
Cavitation Number for Limited
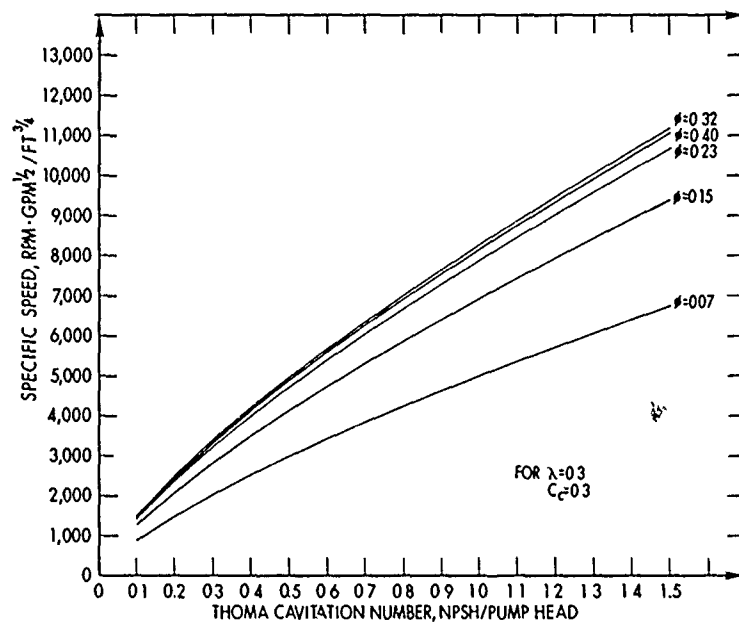Cavitating Designs

Figure 12
Specific Speed Versus Thoma Cavitation Number
for Noncavitating Designs

The pump performance at speeds other than the maximum ship design speed condition can be approximated by:

$$\eta_{Pod} = \frac{K_1 \, Q_{od}^2}{H_{od}} - \frac{K_2 \, Q_{od}^3}{H_{od}^{3/2}} , \tag{42}$$

where

$$K_1 = \frac{3\eta_p \, H_{pd}}{Q_d^2} \tag{43a}$$

and

$$K_2 = \frac{2\eta_p \, H_{pd}^{3/2}}{Q_d^3} , \tag{43b}$$

where η_{Pod} is the pump efficiency at off design speed conditions. The maximum pump efficiency, η_p, for axial and centrifugal pumps is in the 85% to 90% range for well-designed pumps.

SENSITIVITY STUDIES

The effects of various parameters on a wide boundary layer inlet performance were considered for a representative 70-ton, 50-knot planing craft. The craft net thrust requirements versus speed were obtained from equation (21) with a 25% margin for appendages, sea state, and roughness and are plotted in figure 13, where an additional thrust margin equal to 2% of the craft weight is included to allow for acceleration. The base line craft design conditions at 50 knots were taken as:

$$R = 1.8 = \text{jet velocity ratio} = V_j/V_\infty$$

$$\alpha = 0.7 = \text{inlet velocity ratio} = V_i/V_\infty$$

$$L_X = 90 \text{ feet}$$

$$L_W = 12 \text{ feet}$$

$$\eta_p = 85\%$$

$$K_\ell = 0.3$$

$$C_{D_i}/2\alpha = 0.05$$

At the 50-knot design condition, $\delta \approx 7$ inches and $(y/\delta) \approx .4$ at the inlet for the above conditions.
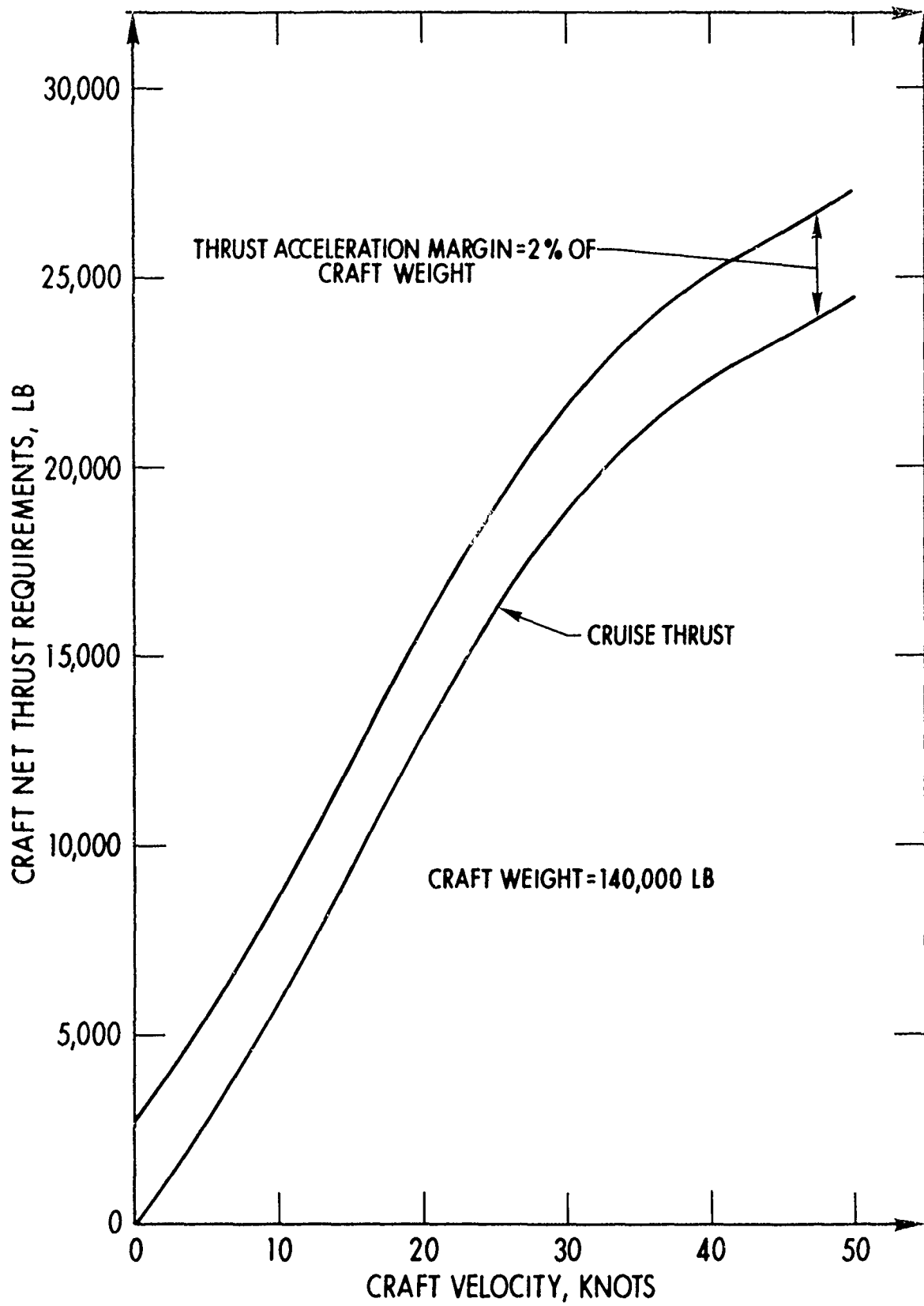
Figure 13
Net Thrust Versus Craft Velocity

Figures 14 and 15 show the effects of craft velocity on inlet and jet velocity ratio, momentum velocity ratio, overall propulsive coefficient, pump efficiency, and horsepower for the cruise and accelerating conditions.
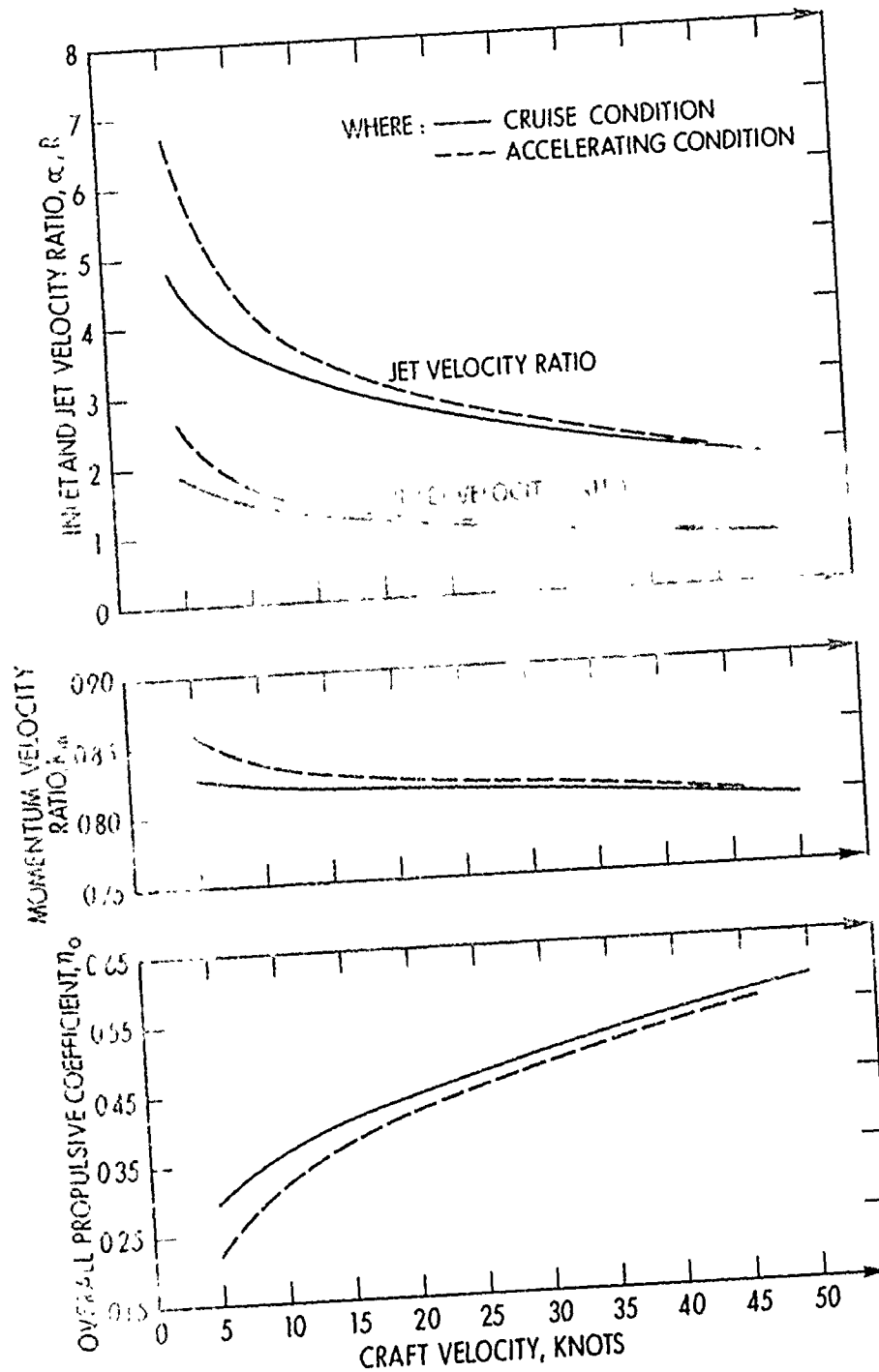

Figure 14
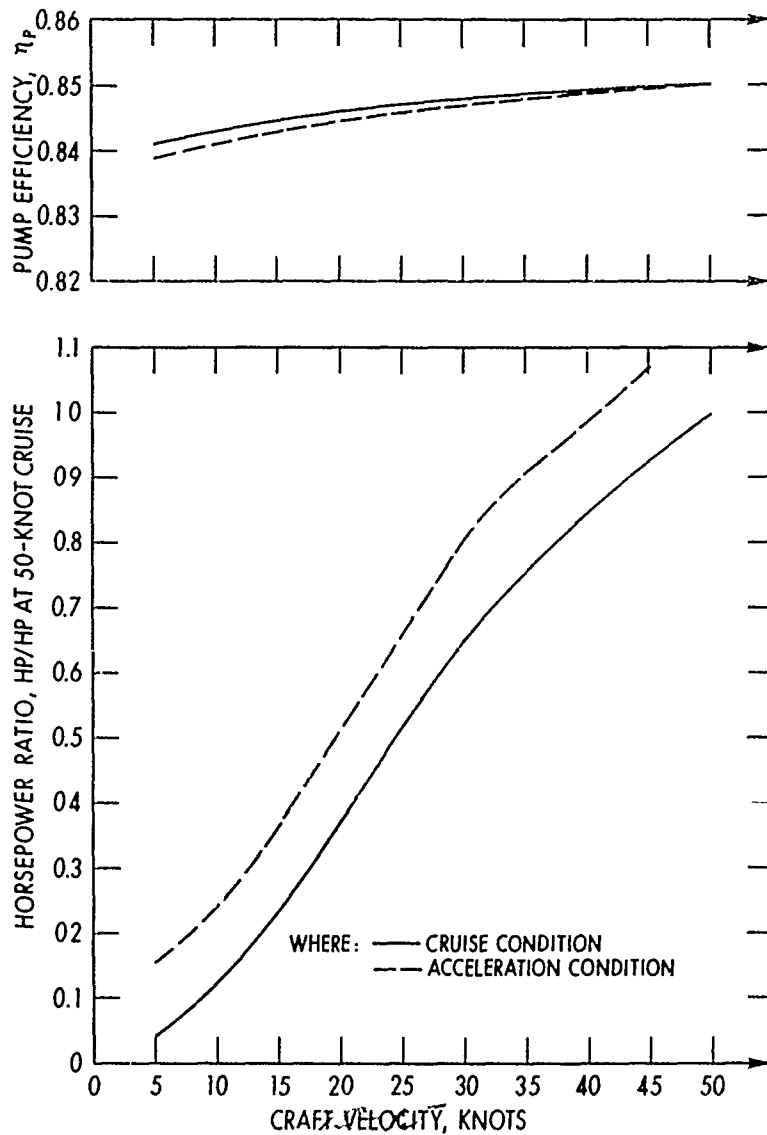Wide Boundary Layer Inlet Performance

24

Figure 15
Wide Boundary Layer Inlet Performance

The effects of craft velocity on the various parameters are as follows:

  ● Jet velocity ratio - increases with decreasing speed, thus making kinetic energy losses proportionally higher.

  ● Inlet velocity ratio - increases with decreasing speed. The $C_{D_i}/2\alpha$ term was considered to be constant with speed in the calculations but might actually decrease with decreasing speed due to the increasing α at lower speed and no great expected changes in C_{D_i}. This would improve low speed efficiency slightly above values shown.

● Momentum velocity ratio - increases slightly with decreasing speed, thus reducing η_O slightly.

● Overall propulsive coefficient - decreases with decreasing speed due mainly to the increasing jet velocity ratio.

● Pump efficiency - is relatively unaffected by craft speed, showing the pump operates close to its optimum over the speed range.

● Horsepower requirements - are reduced with decreasing speed due to the lower thrust requirements. Horsepower requirements vary somewhat linearly with speed. At about half speed, power requirements are thus about half of design speed requirements. Thus, on a ship of two or more engines, one or more could be shut off and the remaining unit or units could be operated at higher power where sfc is generally improved.

Figure 16 shows the effects of wetted length, inlet width, inlet loss coefficient, and drag coefficient on the overall propulsive coefficient. The effects on overall propulsive coefficient are as follows:

● Wetted length - A reduction in wetted length upstream of the inlet causes only slight reductions in η_O, even for large decreases in wetted length. This is important since planing hulls can have reduced wetted surface with increased speed.

● Inlet width - Increasing inlet width will also increase η_O slightly since a smaller percentage of the boundary layer thickness will be used, an effect that results in a lower inlet momentum velocity.

● Inlet loss coefficient - Increasing inlet loss coefficient will cause noticeable decreases in η_O. Keeping inlet losses very small will be difficult due to the following:

. There are losses on the ramp directly upstream on the flush inlet which reduce the inlet dynamic head by roughly 10%[3,4] compared to what would be predicted for the ingested portion of the boundary layer.

. The skewed inlet profile will cause problems in avoiding separation in the inlet diffuser.[4] Separation causes diffuser efficiency to suffer, and undesirable flow patterns are established.

● Inlet drag coefficient - Increasing drag coefficient will significantly reduce η_O, especially since the area of interest is a low jet velocity ratio region. However, very low inlet drag

coefficients are possible with flush inlets.[3,4] The wide
boundary layer inlet will operate in the lower velocity environ-
ment of the boundary layer, resulting in potentially even lower
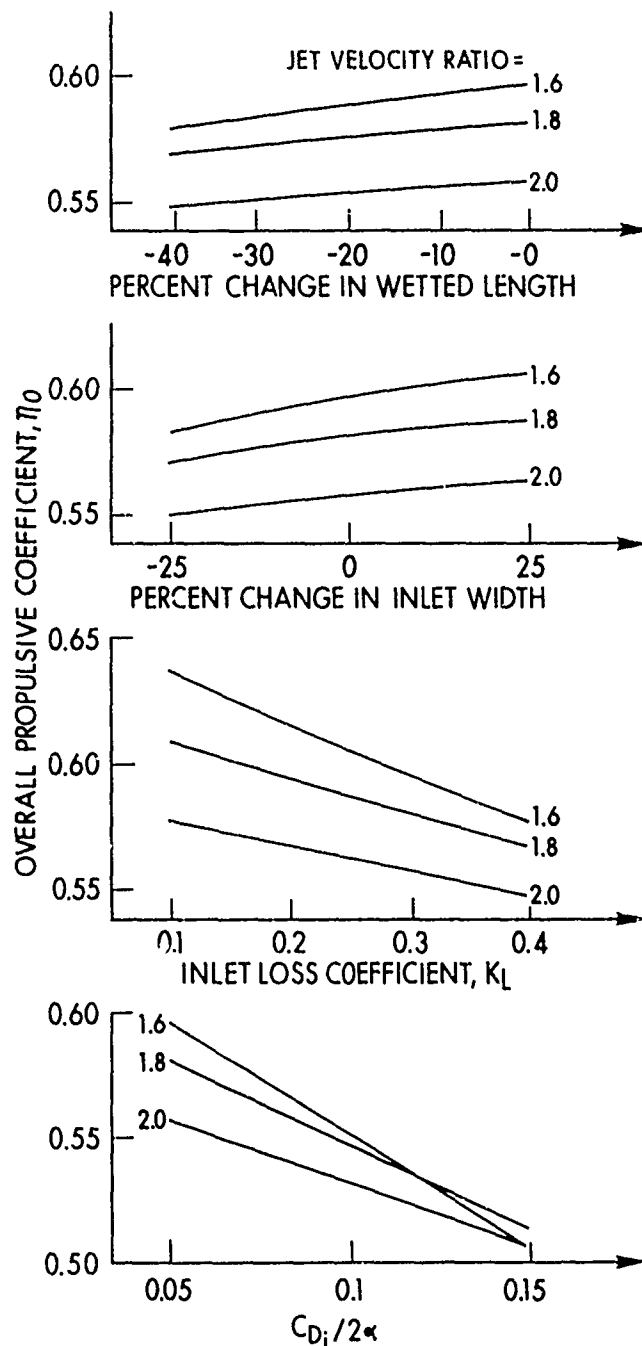inlet drag coefficients.

Figure 16
Effects of Various Parameters on Wide
Boundary Layer Inlet Performance

Figure 17 shows the effects of jet velocity ratio on a wide boundary layer inlet system design at the maximum cruise design speed. The use of low jet velocity ratios (≤ 2) at design speed will most likely be necessary to ensure an η_O high enough to compete with other alternative systems.
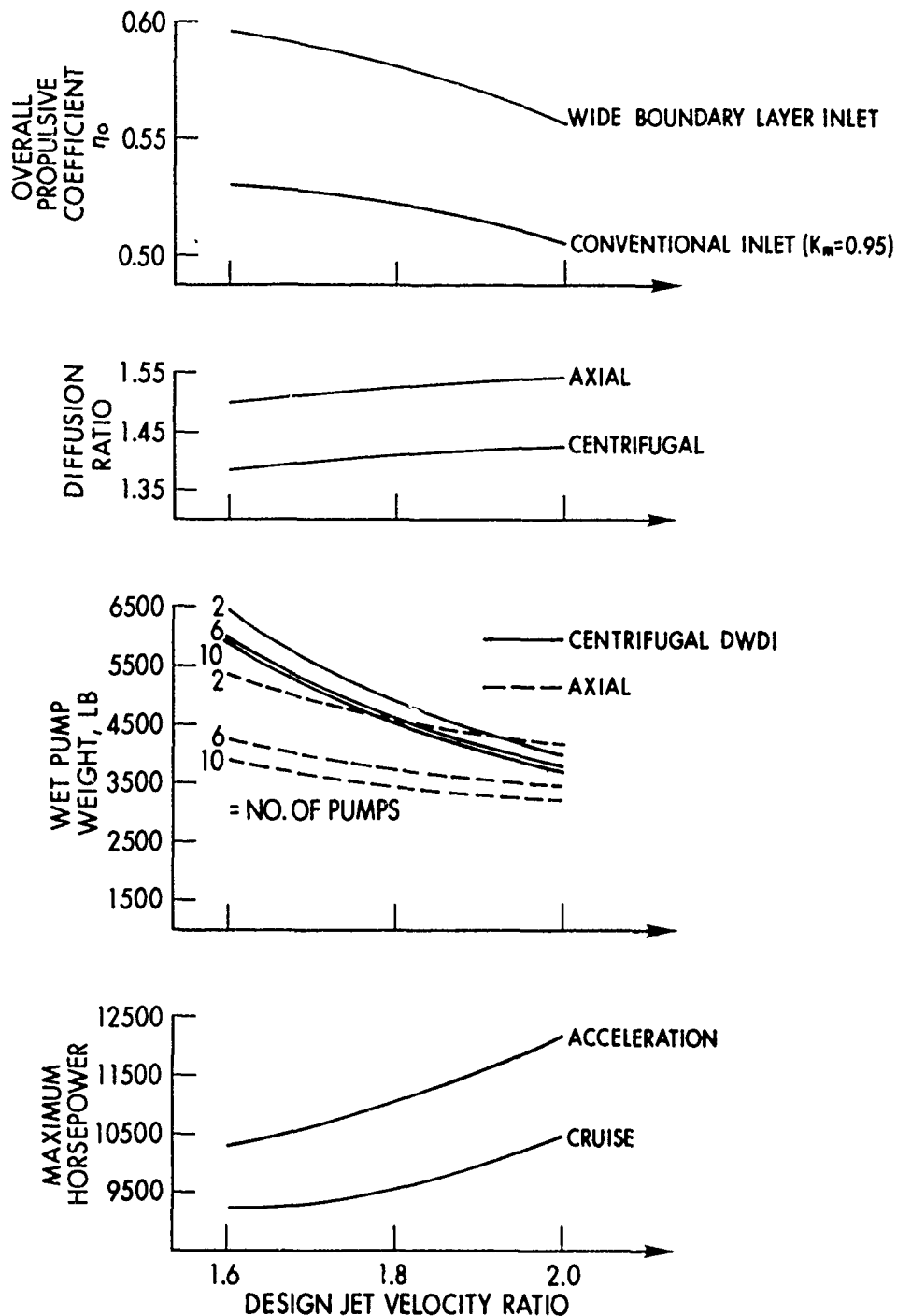

Figure 17 - Effects of Jet Velocity on a
Wide Boundary Layer Inlet Design at
Cruise Conditions

The effects of jet velocity ratio were:

- Overall propulsive coefficient - increases with decreasing jet velocity ratio for the variables investigated. Figure 17 also shows a comparison with what would be expected for a conventional low aspect ratio inlet where boundary layer effects are small and K_m is assumed equal to 0.95. The wide inlet shows a 5- to 6.5-point efficiency advantage over a conventional system. Figures 4 through 6 also show jet velocity ratio effects on η_o for a wider range of variables.

- Diffusion ratios - are low and show a tendency to decrease slightly with reduced jet velocity ratio. The low diffusion ratios result from high flow coefficients appearing desirable. Since diffusion ratios can be low, diffuser size and losses may potentially be kept low.

- Pump weight - increases rapidly with decreasing jet velocity ratio due to the increased pump mass flows. The pump designs are based on noncavitating flow at the craft design speed. Increasing the number of pumps will reduce pump weight. Axial pumps tend to show a weight advantage over centrifugal pumps; but when the complete system is considered, this advantage may vanish.

- Maximum horsepower - increases with increasing jet velocity ratio due to higher jet kinetic energy losses.

EVALUATION OF POTENTIAL WIDE INLET
PUMP SYSTEM ARRANGEMENTS

Three different pump arrangements were investigated for a 70-ton planing craft:

- Multiple parallel DWDI centrifugal pumps.

- Multiple parallel axial pumps with turning volutes.

- Conventionally mounted axial pumps.

The three arrangements are shown in figures 18 through 20, respectively. In all three cases, the pumps are driven by two gas turbines. However, the first two arrangements can declutch a turbine to provide improved fuel consumption at lower speed and power conditions. The weight of a combining gear on the conventionally mounted axial pumps was too high in this case to be considered for use.

The multiple parallel DWDI centrifugal pump arrangement, figure 18, is attractive since the pumps can be strung on a single shaft. The multiple pump inlets are then in a line which will closely match the inlet width. This will enable the inlet diffusion to be essentially two-dimensional and should keep losses to a minimum. The multiple small diameter pumps should help keep pump weight and elevation losses to a minimum.
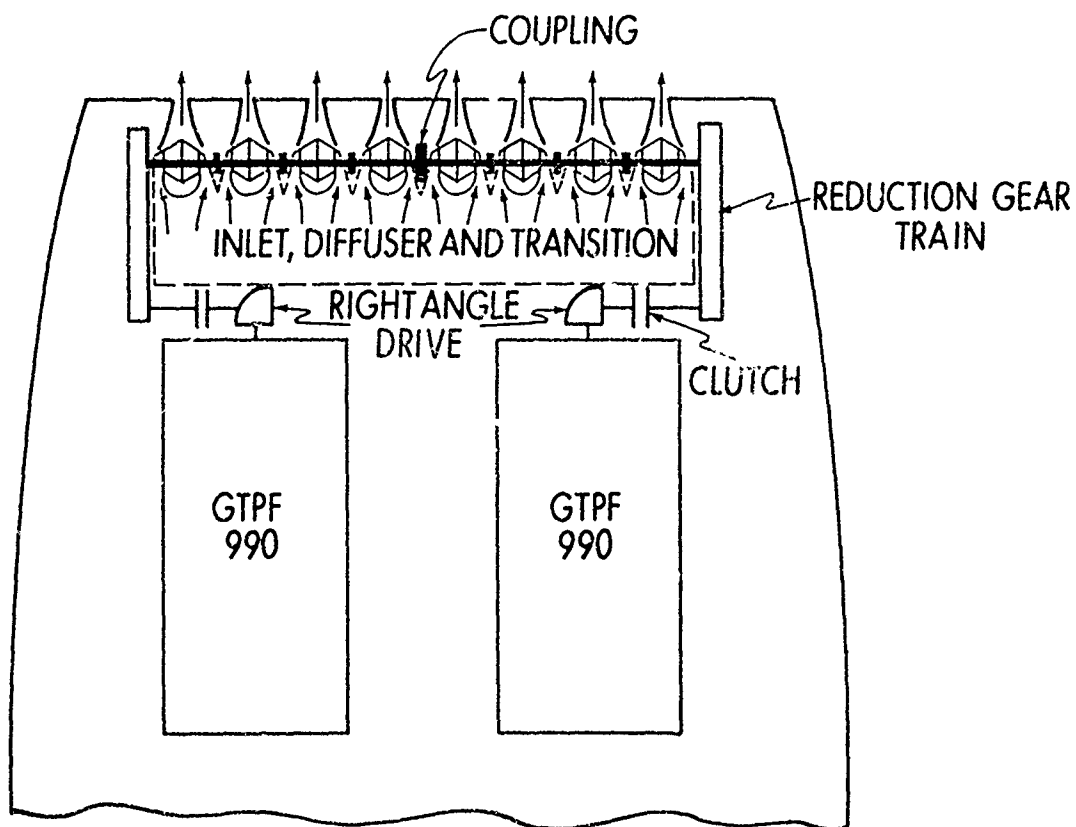

Figure 18
Multiple Parallel Double Width,
Double Inlet Centrifugal
Pump Arrangement

The multiple parallel axial pumps' arrangement of figure 19 enables all the pumps to be mounted on a common shaft. The flow must be turned (turning losses were considered) to get into the pump, and a turning volute is required downstream of the pump to direct the flow toward the transom with minimum losses. This arrangement strings the pumps out to match the inlet width more effectively. The small pump diameters should keep pump weight low. Pump weight has been increased by one-third to account for the turning volute.

COUPLING

REDUCTION GEAR
TRAIN

INLET, DIFFUSER AND TRANSITION

RIGHT ANGLE
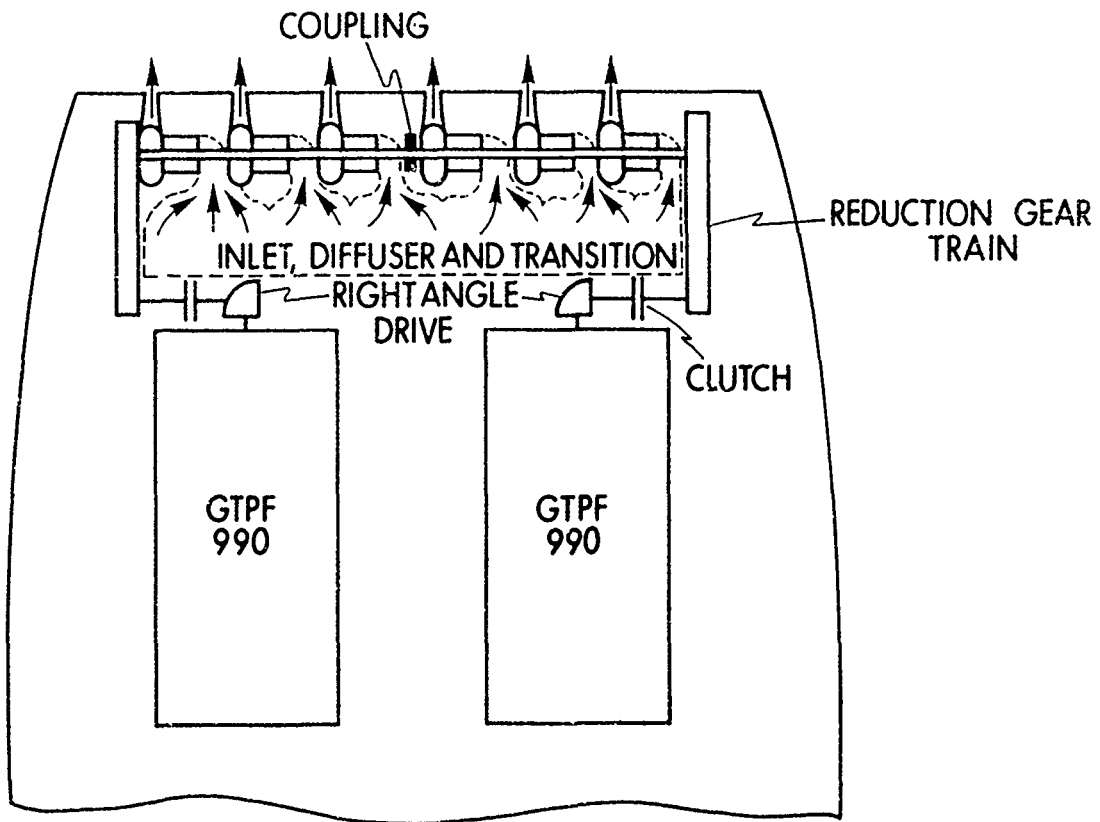DRIVE

CLUTCH

GTPF
990

GTPF
990

Figure 19
Multiple Parallel Axial Pumps With
a Turning Volute

The conventionally mounted axial pumps' arrangement of figure 20 enabled the realization of a simple compact system. The flow from the wide inlet, however, must be ducted to the narrower pump inlet which will require three-dimensional diffusion and/or transition with their associated losses in a minimum length inlet system to minimize weight.
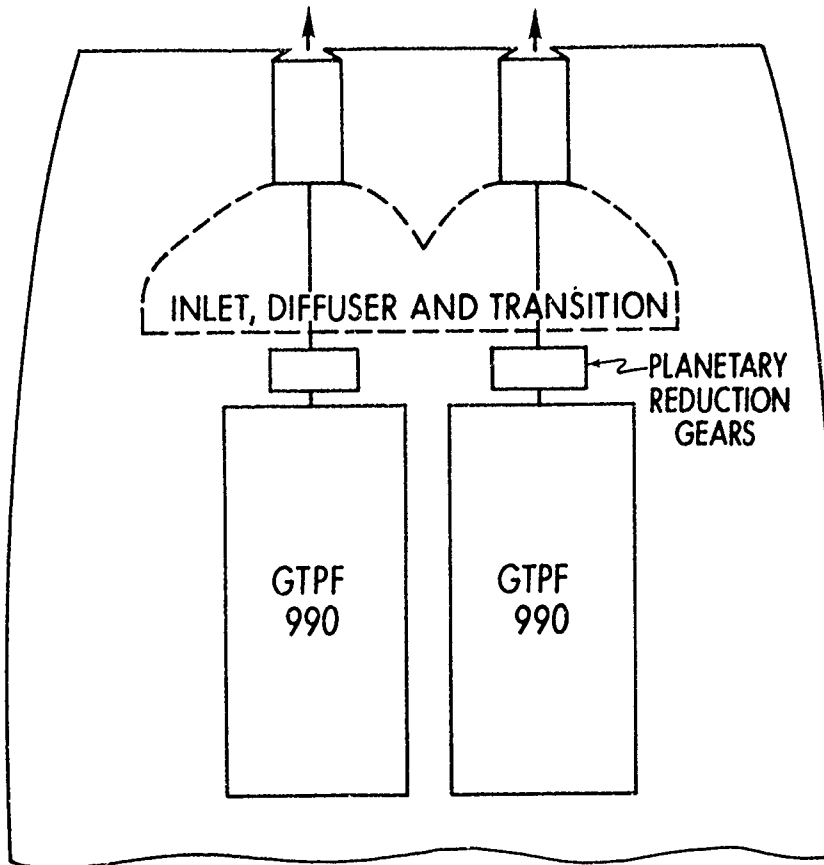

Figure 20
Conventionally Mounted Axial Pumps

The craft drag characteristic was assumed to be the same as shown in figure 13. The basic craft design conditions were as follows:

$$W_c = 70 \text{ tons}$$

$$V_\infty = 50 \text{ knots (maximum)}$$

$$R = 1.8 \text{ (at 50-knot cruise)}$$

$$\alpha = 0.7 \text{ (at 50-knot cruise)}$$

$$L_x = 90 \text{ feet}$$

$$L_w = 12 \text{ feet}$$

$$\eta_p = 0.85$$

$$K\text{-factor} = 500$$
gears

Duct weight = 15 psf of surface

On all the designs it was assumed that after the inlet there would be a length of constant area duct with area equal to the inlet cross section and running a minimum of five inlet heights. This would allow the skewed boundary layer inlet profile to become more uniform before any diffusion took place. Since the amount of diffusion required in the designs considered turned out to be small, this duct length did not involve any weight penalty. Additional duct would have been required to get to the pump inlet due to the short diffusers.

The two multiple parallel pump arrangements have similar gear arrangements. Power from the gas turbine is fed to a 1:1 right angle bevel gearbox whose output then drives a reduction gear train. This arrangement appears very desirable since it allows flexibility in where to mount the gas turbines. Also the reduction gear train enables offset so that the input shaft clears the pump and ducting. Most important, the reduction gear train is half the width of any other alternative systems, thus allowing maximum utilization of transom width for stringing out the multiple pumps to match the inlet width.

The following tabulation is a comparison of the three arrangements. The weights of the transmission system, including shafting, bearings, etc, were based on Muench.[11] The tabulation shows that the centrifugal and conventionally mounted axial pumps yield comparable system weights. The multiple parallel axial arrangement was much heavier due to the additional weight of the turning volutes and heavier reduction gears. System losses were assumed to be slightly higher for the axial pump arrangements so they had increased horsepower requirements which appears likely due to their required inlet and/or outlet ducting configurations. The centrifugal pump arrangement appears to offer the most advantages since, in addition to having a weight comparable to the conventional axial arrangement, all the centrifugal pumps can be run from a single gas turbine to improve low power sfc. A combining reduction gear was estimated to add about 3200 more pounds to the conventional axial pump setup. Further study, particularly in the area of system losses, would be needed to assure the selection of the appropriate pump and arrangement.

COMPARISON OF PUMP ARRANGEMENTS

	Multiple Parallel DWDI Centrifugal Pumps	Multiple Parallel Axial Pumps With Turning Volutes	Conventionally Mounted Axial Pumps
No. of pumps	8	6	2
Impeller exit tip velocity, fps	157.5	112.7	112.7
Pump flow coefficient	0.40	0.35	0.35
Inlet axial velocity, fps	43.0	39.5	39.5
Inlet loss coefficient	0.3	0.35	0.35
Inlet height, in.	2.59	2.59	2.59
Inlet momentum velocity ratio	0.797	0.797	0.797
η_o (cruise)	0.581	0.574	0.574
HP_{max}	10,972	11,205	11,205
HP_{cruise}	9,508	9,731	9,731
Diffusion ratio	1.41	1.56	1.56
Pump diameter, ft	0.862 o.d. x 0.597 i.d.	0.97	1.64
Shaft blockage coefficient	0.43	0.31	0.22
Pump maximum rpm	3,490	2,212	1,310
Pump unit length, ft	12.07	13.39	3.28 ea.
Reduction gear ratio	4.87	7.68	12.98
Wet pump weights	4,555	5,083	4,704
Inlet weight, lb	574	574	574
Diffuser and transition weights, lb	313	486	769
Pump inlet elbow weights, lb	*	284	–
Bevel gear weights, lb	1,240	1,240	–
Reduction gear weights, lb	1,690	3,174	2,636
Weights of shafts, bearings, clutches, etc, lb	589	574	311
Weight of gas turbines, lb	6,402	6,402	6,402
Propulsion system weight, lb	15,363	17,817	15,396
Propulsion system weight fraction	0.110	0.127	0.110
Propulsion system specific weight, lb/hp	1.400	1,590	1.374

*Included in pump weight.

CONCLUSIONS

The use of wide boundary layer inlets should enable realization of improved propulsive coefficients for water-jet systems. This type of inlet is most applicable to displacement-type craft, which have sufficiently wide beam to accommodate it. Propulsion coefficients approaching 0.6 are predicted, with improvements being about 10% to 12% above those of conventional inlets. The biggest improvements in propulsive coefficient for a wide inlet system occur for low design jet velocity ratios on the order of 1.6 to 2.0. As jet velocity ratio increases, the effect of reduced inlet momentum coefficient is minimized and wide inlet performance approaches that of a conventional flush inlet. Thus, wide inlet systems are most applicable to a craft that spends a large percent of its time at or near its design jet velocity ratio.

The performance of a wide boundary layer inlet system is most affected by increasing inlet drag, inlet system losses, and jet velocity ratio. Changes in wetted length and inlet width have a lesser effect on overall system efficiency. The multiple parallel centrifugal pumps and the conventionally mounted axial pumps both appear to have potential application on a wide boundary layer inlet system. In this study the centrifugal setup had low speed powering advantages which could only be obtained in the axial arrangement through increased gear weight.

RECOMMENDATIONS

● Model testing of a wide inlet system is needed to determine inlet system losses, drag coefficients, and potential air ingestion problems.

● Measurements of boundary layer thickness and profile on planing and displacement craft, especially at high speeds, are needed to assure that the reduced velocity which is characteristic of the boundary layer is present in spite of the induced ventilation and broaching that occur during nonideal sea states.

TECHNICAL REFERENCES

1 - Burke, F. P., et al, "R & D Testcraft: XR-1B Semi Flush Inlets, Final Test Report," Rohr Industries, Inc., Rept RHR-72-941 (Oct 1972)
2 - Burke, F. P., et al, "R & D Testcraft: XR-1B Semi Flush Inlets, Correlation Report," Rohr Industries, Inc., RHR-72-642 (Dec 1972)
3 - Johnson, V. E., et al, "Design and Performance of Diffusers, Fixed-Area Inlets and Variable-Area Inlets in Integrated Inlet-Diffuser Subsystems," Hydronautics, Inc., Rept 7152-1 (Aug 1972)

4 - Stephens, L. K., et al, "Waterjet Inlet/Duct Development Phase I, Validation Tests," Hydronautics, Inc., Rept 7244-1 (Jan 1973)

5 - Poquette, G. M., and R. J. Etter, "Waterjet Inlet/Duct Development Phase II, XR-1B Correlation Tests," Hydronautics, Inc., Rept 7244-2 (Mar 1973)

6 - Barr, R. A., "State-of-the-Art Technology and Performance Prediction Methods for Waterjet Propulsion Systems for High Speed Naval Ships," Hydronautics, Inc., Rept 7224-7 (June 1974)

·7 - Brophy, M. C., "A Theoretical Study of Cavitating Inducers with an Application to Waterjet Propulsion," NSRDC Rept 4431 (Feb 1975)

8 - Gongwer, C. A., "A Theory of Cavitation Flow in Centrifugal Pump Impellers," Trans. of the ASME (Jan 1941)

9 - Carmichael, A. D, and R. C. Percival, "Design Optimization of Waterjet Propulsion Systems for Hydrofoils, Part 3," MIT Ocean Engineering Rept 72-15 (1972)

10 - Wislicenus, G. F., Fluid Mechanics of Turbomachinery, Vol. 1, New York, Dover Publications, Inc. (1965)

11 - Muench, R. K., "Arctic Surface Effect Vehicle Program: Parametric Data on a Mechanical Transmission Suitable for Large Surface Effect Vehicles," NSRDC Rept 27-650 (Dec 1973)

PAS-75-45   36

Copies			Copies	
9	NAVSEA		1	The Boeing Co.
	1 (SEA 03C)			Seattle, Wash.
	2 (SEA 032)			(R. Dixon)
	2 (SEA 0331G)*			
	2 (SEA 035)		1	Dr. G. F. Wislicenus
	2 (SEA 09G32)			4641 E. Coronado Dr.
				Tucson, Ariz. 85718
2	NAVSEC			
	1 (SEC 6144, Blount)			
	1 (SEC 6661, Lombardi)			

CENTER DISTRIBUTION

Copies		Code
12	DDC	1 (1170)
		2 (15)
2	Aerojet Liquid Rocket Co.	2 (1532)
	P.O. Box 13222	15 (2721)
	Sacramento, Calif. 95813	1 (5222)
	(R. G. Sjogren)	2 (5231)
		1 (9431B)

2   Applied Research Lab.
P.O. Box 30
State College, Pa. 16801
(W. Gearhart)
(R. E. Henderson)

2   Hydronautics, Inc.
7210 Pindell School Rd.
Laurel, Md. 20810
(R. Barr)
(R. Etter)

1   Massachusetts Institute
of Technology
Dept. of Ocean Engr.
Cambridge, Mass. 02139
(Dr. A. D. Carmichael)

2   Rocketdyne
6633 Canoga Ave.
Canoga Park, Calif. 91304
(G. Wong)
(L. Barham)

*Addressee.

PAS-75-45, March 1976